

Passive vibration control of plan-asymmetric buildings using tuned liquid column gas dampers

Chuan Fu[†]

*College of Architecture, North China University of Technology, Beijing 100144, China
Center of Mechanics and Structural Dynamics, Vienna University of Technology,
Vienna 1040, Austria-Europe*

(Received January 20, 2009, Accepted August 14, 2009)

Abstract. The sealed, tuned liquid column gas damper (TLCGD) with gas-spring effect extends the frequency range of application up to about 5 Hz and efficiently increases the modal structural damping. In this paper the influence of several TLCGDs to reduce coupled translational and rotational vibrations of plan-asymmetric buildings under wind or seismic loads is investigated. The locations of the modal centers of velocity of rigidly assumed floors are crucial to select the design and the optimal position of the liquid absorbers. TLCGD's dynamics can be derived in detail using the extended non-stationary Bernoulli's equation for moving reference systems. Modal tuning of the TLCGD renders the optimal parameters by means of a geometrical transformation and in analogy to the classical tuned mass damper (TMD). Subsequently, fine-tuning is conveniently performed in the state space domain. Numerical simulations illustrate a significant reduction of the vibrations of plan-asymmetric buildings by the proposed TLCGDs.

Keywords: asymmetric building; Bernoulli's equation; gas-spring effect; sealed absorber; modal tuning; state space optimization.

1. Introduction

The current trend towards buildings of ever increasing heights and the use of light-weight, high-strength materials and advanced construction techniques have led to increasingly flexible and lightly damped structures. The tuned liquid column dampers (TLCDs) as cost-effective, passive energy substructures substitute the tuned mechanical dampers (TMDs), either of the spring-mass-dashpot or of the pendulum-dashpot type, in order to increase the effective structural damping and reduce the ductility demands in the response to dynamic loads like earthquakes and various kinds of wind excitation. Such a TLCD consists of a rigid, U-shaped tube of rectangular, oval or circular cross-section that is smoothly integrated into a building and partially filled with a liquid, preferably water. Sakai 1989 and Hitchcock 1997 applied TLCD to tall buildings. However, the natural frequency of a properly sized, i.e., for civil engineering applications properly sized TLCD is limited to frequencies below 0.5 Hz. Hochrainer 2001 invented the gas-spring effect in a novel sealed design of the TLCGD, namely TLCGD to overcome this low frequency problem and mitigate wind- and earthquake excited vibrations of tall buildings (Hochrainer and Ziegler 2006) with in-plane

[†] E-mail: fu.chuan79@gmail.com

(horizontal) translational natural modes. Reiterer 2004, Reiterer and Ziegler 2004 applied the TLCGD to mitigate coupled flexural and torsional vibrations of long-span bridges under traffic loads. Since both vertical and torsional forcing render parametric excitation of the fluid flow, Reiterer and Ziegler 2006 presented the cut-off values of the damping of the fluid flow to surely avoid any undesirable disturbance of the TLCGD damping effects. The fluid stroke reaches the meter-range for small fluid-structural mass ratios. Therefore, the frequency range of application must be limited to keep the relative maximum fluid speed below about 10 m/s for the sake of keeping the fluid-gas interface intact and to avoid the dynamic contact angle to reach 180° , Lindner-Silvester and Schneider 2005.

A real building usually possesses a large number of degrees of freedom and is actually asymmetric to some degree even with a nominally symmetric plan. It will undergo coupled vibrations simultaneously under purely translational excitations. The coupled, modal displacements and the small rotation combine approximately to a rotation about the floor's modal center of velocity, see e.g., Ziegler 1998, page 14. If such a modal center of velocity falls outside of the floor plan, the translation dominates. Consequently, the ideal position of the trace of the mid-plane of the U- or V-shaped TLCGD requires its normal distance from this center to be maximum. Tuning of the TLCGD in the design stage is performed in several steps. At first, the linearized model is tuned with respect to a selected mode of the structure using the analogy to TMD tuning (Hochrainer 2005) with the properly transformed Den Hartog's optimal parameters taken into account (Den Hartog 1956). In a second step, improvements of the performance in multiple-degree-of-freedom (MDOF) structures are achieved by subsequently considering the neighbouring modes as well in a state space representation and minimizing the weighted squared area of the frequency response function (FRF), with the Den Hartog parameters serving as the initial values. Such a fine-tuning renders the optimal parameters modified. Final adjustments are easily performed in the course of *in-situ* testing by adjusting the equilibrium gas pressure in the TLCGD. Optimal damping of the fluid flow may require an orifice plate built in the piping system. The numerical simulations are presented to demonstrate the new design procedure and lateral-torsional control effectiveness of the spatially placed TLCGDs system with fairly small mass ratios assigned.

2. Modal center of velocity C_V

The N-storey building is ideally modelled as a structure comprising of members connected by rigid floors, it has three degrees of freedom at each floor using static condensation, i.e., lateral displacements of center of mass C_M with respect to the foundation and the rotational angle about the vertical x -axis. For floor i , they are denoted v_i and w_i , and θ_i . The orthogonal modal shape vectors $\vec{\phi}$ by solving the eigenvalue problem of the undamped structure are considered to determine the position of the modal center of velocity.

The point of a rigid body in-plan motion that instantly has zero velocity is called the center of velocity C_V . The modal displacements and rotation combine kinematically to a sufficiently small rotation about the floor's center of velocity. The modal center of velocity of a floor is indicated in Fig. 1. The coordinates of the modal center of velocity of the i -th floor in the j -th mode, C_{vij} can be derived in terms of the components of the modal vector $\vec{\phi}_j$, Ziegler 1998, page 19,

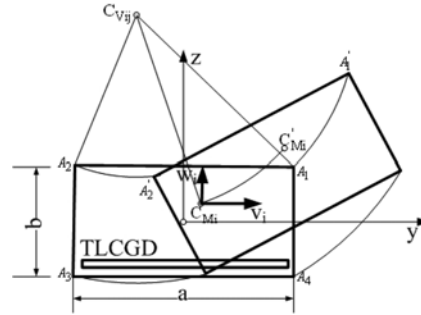


Fig. 1 Asymmetric space-frame, small rotation $|\theta| \ll 1$ of the floor is understood; exaggerated in the figure

$$y_{C_{Vij}} = y_{C_{Mi}} - \frac{r_{Si}}{\phi_{j3i}} \phi_{j(3i-1)}, \quad z_{C_{Vij}} = z_{C_{Mi}} + \frac{r_{Si}}{\phi_{j3i}} \phi_{j(3i-2)}, \quad \phi_{j3i} \neq 0 \quad (1)$$

where r_{Si} denotes the radius of inertia with respect to the floor's center of mass.

The position of the center of velocity falls outside of the geometrically regular floor plan in Fig. 1, translation of the floor dominates, thus a U- or V-shaped TLCGD can be installed parallel to the y -axis at the lower edge of the floor, $z = -b/2$, rendering the normal distance of its trace to C_V as large as possible to enhance the damping efficiency and compatible to the geometric floor plan. If the center of velocity lies inside of the floor plan, rotation dominates the translations. A novel (torsional) TTLCGD should be installed, but is not discussed further in this context, Ziegler and Fu 2007, Fu 2008.

3. U- or V-shaped tuned liquid column-gas damper

A tuned liquid column-gas damper (TLCGD) is a symmetric, U- or V-shaped rigid and sealed piping system consisting of one horizontal and two inclined ($\pi/4 < \beta \leq \pi/2$), partially fluid-filled pipe sections, see Fig. 2. The ends of the piping system are sealed and filled with gas, contrary to the classical TLCD design, such that an internal gas pressure can build up on either side of the liquid path, denoted p_1 and p_2 with a common reference equilibrium pressure p_0 . B and H denote the horizontal length of the liquid column and the length of the liquid column in the inclined pipe sections at rest. Furthermore A_B , A_H denote the horizontal and inclined cross-sectional areas, the fluid volume is $2HA_H + BA_B$. The relative motion of the liquid column is described by the displacement $u(t)$.

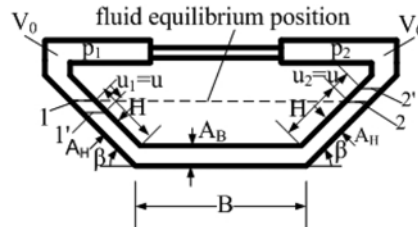


Fig. 2 U- or V-shaped tuned liquid column gas damper, symmetric design as a framed structure. One-sided gas volume $V_0 = A_H H_a$ above fluid-gas interface 1, sealed

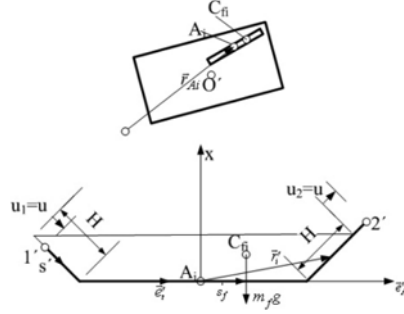


Fig. 3 TLCGD in horizontal general motion. Unit vector \vec{e}'_{Ai} in direction of its trace. Instant position of the fluid mass center C_{fi} marked

3.1 The equation of relative motion of the fluid in a TLCGD, attached to the selected floor number i

Let a TLCGD be installed on the i -th floor of the N -storey asymmetric building, its trace in the floor is oriented by the angle γ to y -direction and the reference point $A_i(y_{Ai}, z_{Ai}, 0)$. The equation of the ideal fluid flow in the rigid pipe system is derived by the generalized non-stationary Bernoulli equation, see Fig. 3, Ziegler, 1998, page 497.

$$\int_{1'}^{2'} \vec{a}_i \cdot \vec{e}'_i ds' = -g(x_2 - x_1) - \frac{1}{\rho}(p_2 - p_1) \quad (2)$$

where x_1 , x_2 , g and ρ denote the geodesic height of the free surface $1'$ and $2'$ in Fig. 2, the constant of gravity $g = 9.81 \text{ m/s}^2$ and the liquid density, e.g., of water $\rho = 1000 \text{ kg/m}^3$. \vec{e}'_i denotes the relative streamline's tangential direction. The absolute acceleration of a fluid particle \vec{a}_i is delineated into the guiding acceleration, the Coriolis component and the relative acceleration. Since the Coriolis acceleration $\vec{a}_{ci} = 2\dot{\theta}_i \vec{e}_x \times \vec{u}$ is orthogonal to the relative velocity \vec{u} , it does not at all contribute to the Eq. (2). The relative acceleration $\vec{a}' = d'\vec{u}/dt$ is the relative rate of the relative velocity and with respect to the moving frame can be expressed as $\vec{a}' \cdot \vec{e}'_i = \partial' \dot{u} / \partial t + \partial / \partial s' (\dot{u}^2 / 2)$. The guiding acceleration in tall buildings reduces, $\vec{r}'_{y'z'i}$ is the horizontal component of the relative position of a fluid particle \vec{r}'_i with respect to point A_i , see Fig. 3,

$$\vec{a}_{gi} = \vec{a}_{Ai} + \ddot{\theta}_i \vec{r}'_{y'z'i} - \dot{\theta}_i^2 \vec{r}'_{y'z'i}, \quad \vec{r}'_{y'z'i} = \vec{e}_x \times \vec{r}'_{y'z'i} \quad (3)$$

The absolute acceleration of the reference point $A_i(y_{Ai}, z_{Ai}, 0)$ projected in \vec{a}'_{Ai} -direction is given by, Fig. 4,

$$\vec{a}_{Ai} \cdot \vec{e}'_{Ai} = a_{yi} \cos(\gamma + \theta_i) + a_{zi} \sin(\gamma + \theta_i)$$

$$a_{yi} = \ddot{v}_g + \ddot{v}_i - (z_{Ai} - z_{C_{Mi}}) \ddot{\theta}_i - (y_{Ai} - y_{C_{Mi}}) \dot{\theta}_i^2, \quad a_{zi} = \ddot{w}_g + \ddot{w}_i - (y_{Ai} - y_{C_{Mi}}) \ddot{\theta}_i - (z_{Ai} - z_{C_{Mi}}) \dot{\theta}_i^2 \quad (4)$$

If the piping system is sealed, the gas is quasi-statically polytropically compressed, Ziegler 1998, page 88 by the liquid surface in sufficiently slow motion (piston theory). Hence, the gas pressure difference $p_2 - p_1$ in Eq. (2) in the range of linearized gas compression, i.e., if the maximum fluid-stroke is limited by $\max|u| \leq H_g/3$, is approximated by

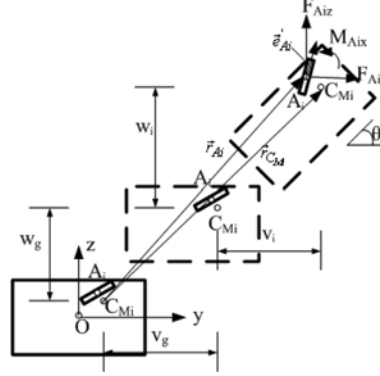


Fig. 4 TLCGD under general in-plane acceleration of the floor: \dot{v}_i, \dot{w}_i and $\dot{\theta}_i$. Resulting force components F_{Aiy} , F_{Aiz} and moment M_{Aix} , indicated in the instant configuration

$$p_2 - p_1 \approx 2np_0u/H_a, \quad 1 \leq n \leq 1.4, \quad V_0 = A_H H_a \quad (5)$$

H_a denotes the effective height of the symmetric left and right gas volumes at rest, Fig. 2. Performing the integration of the non-stationary term in Eq. (2), and considering the guiding acceleration as of Eqs. (3) and (4) assigned, and further, adding the experimentally observed averaged turbulent damping $\delta_L |\dot{u}| \dot{u}$ to the right hand side of Eq. (2) yields the equation of relative fluid motion in a TLCGD under the base excitation, where $\delta_L = \lambda/2L_{eff}$ is the head loss coefficient, for detailed derivations see Fu 2008,

$$\ddot{u} + \delta_L |\dot{u}| \dot{u} + \omega_A^2 \left(1 - \kappa_1 \frac{\dot{\theta}_i^2}{\omega_A^2} \right) = -\kappa (\vec{a}_{Ai} \cdot \vec{e}'_{Ai}) \quad (6)$$

Where the geometry dependent excitation influence factors κ , κ_1 and the effective length L_{eff} of the liquid column are defined by

$$\kappa = \frac{B + 2H \cos \beta}{L_{eff}}, \quad \kappa_1 = \kappa \cos \beta, \quad L_{eff} = 2H + \frac{A_H B}{A_B} \quad (7)$$

The undamped linear natural circular frequency of TLCGD includes the gas-spring effect due to sealed tubes and is given by

$$\omega_A = \sqrt{\frac{2g}{L_{eff}} \left(\sin \beta + \frac{h_0}{H_a} \right)}, \quad h_0 = np_0 / \rho g, \quad \omega_A = \sqrt{\frac{g}{L_0}} \text{ (mathematical pendulum)} \quad (8)$$

The natural frequency of the “open” TLCD is dependent on the geometry (angle of inclination β and effective liquid column length L_{eff}). Obviously the natural frequency of the TLCD is thus practically limited to frequencies below 0.5 Hz, see Hochrainer 2001. Nevertheless, to extend the frequency range of application a sealed piping system with gas pressure in the equilibrium state is properly adjusted. Equilibrium gas pressure p_0 and the polytropic exponent n are combined in the pressure head h_0 , the new most important frequency tuning parameter. In some applications the atmospheric pressure $p_0 = 1000$ hPa might be still a suitable choice. Similarly to the equivalent (linear) mathematical pendulum of length L_0 , we can determine the parameters of the gas-spring for the same linear absorber frequency, $h_0/H_a = L_{eff}/2L_0 - \sin \beta$.

In the course of the tuning procedure, the nonlinear turbulent damping term δ_L in Eq. (6) has to be transformed into the equivalent linearized viscous damping ζ_A . Demanding equally dissipated energy during one cycle $\zeta_A = (4/3\pi)\max|u|\delta_L$ is given in Eq. (9). Rotational angles are assumed to be small, $|\theta| \ll 1$, thus Eq. (6) takes on its linearized form,

$$\ddot{u} + 2\zeta_A \omega_A \dot{u} + \omega_A^2 u = -\kappa \{ [\ddot{v}_g + \ddot{v}_i - (z_{A_i} - z_{C_{M_i}}) \ddot{\theta}_i] \cos \gamma + [\ddot{w}_g + \ddot{w}_i + (y_{A_i} - y_{C_{M_i}}) \ddot{\theta}_i] \sin \gamma \} \quad (9)$$

The vertical floor acceleration, expected to be present in seismic excitation and commonly equals the vertical component of the ground acceleration, \ddot{V}_g , adds parametric forcing in Eq. (6) in addition to the rotational excitation indicated, $\omega_A^2 u \ddot{V}_g/g$. However, with sufficient damping understood, parametric resonance does not occur, for detailed experimental and numerical investigations see Reiterer and Ziegler 2004. If this linear damping coefficient of the relative fluid flow, ζ_A exceeds the cut-off value of critical parametric resonance at double frequency, the influence of parametric excitation apparent in Eq. (6) becomes fully negligible, with respect to the

vertical seismic excitation $\zeta_A > \zeta_{A,0} = \frac{\ddot{V}_g/g}{4(1 + h_0/H_q \sin \beta)}$ and torsional motion.

3.2 Control forces of TLCD

To couple the TLCD with the main structure it becomes important to know the interface reactions. Assuming that the dead weight of a rigid piping system has been added to the corresponding floor mass, only the interaction forces and moment between the massless, rigid, liquid filled piping system and the supporting floor are determined. Conservation of momentum of the fluid mass m_f , locate C_f in Fig. 3 can be successfully applied to determine the reaction forces F_{Aiy} and F_{Aiz} , they are simplified under the condition $|\theta| \ll 1$ and the essential linear parts become (acting on the piping system),

$$\begin{aligned} F_{Aiy} &= m_f [\ddot{v}_g + \ddot{v}_i - (z_{A_i} - z_{C_{M_i}}) \ddot{u}_{Ti}/r_{Si}] + \bar{\kappa} m_f \ddot{u} \cos \gamma \\ F_{Aiz} &= m_f [\ddot{w}_g + \ddot{w}_i - (y_{A_i} - y_{C_{M_i}}) \ddot{u}_{Ti}/r_{Si}] + \bar{\kappa} m_f \ddot{u} \sin \gamma, \quad u_{Ti} = \theta_i r_{Si} \end{aligned} \quad (10)$$

The following additional geometry coefficients are given by

$$\bar{\kappa} = \kappa L_{eff}/L_1, \quad L_1 = 2H + \frac{A_B}{A_H} B \quad (11)$$

In Eq. (10) $m_f = \rho A_H L_1$ defines the total mass of the moving liquid, and L_1 is a length dependent from the cross section, which becomes equal to L_{eff} in the case of $A_H = A_B$. Conservation of the angular momentum with respect to the accelerated reference point A_i renders the undesired axial moment, after linearization, $|\theta| \ll 1$ is assumed, it becomes (acting on the piping system),

$$M_{Aix} = m_f \bar{\kappa}_3 H^2 \ddot{u}_{Ti}/r_{Si} \quad (12)$$

where the geometry coefficient $\bar{\kappa}_3$ due to rotation is given by

$$\bar{\kappa}_3 = \frac{2H}{L_1} \left[\left(\frac{B}{2H} \right)^2 + \frac{A_B}{3A_H} \left(\frac{B}{2H} \right)^3 + \frac{B}{2H} \cos \beta + \frac{1}{3} \cos^2 \beta \right] \quad (13)$$

The components of the control forces should be statically reduced to the center of mass C_{M_i} , $M_{C_{M_i}x} = M_{Aix} - F_{Aiy}(z_{A_i} - z_{C_{M_i}}) + F_{Aiz}(y_{A_i} - y_{C_{M_i}})$, for the neglected nonlinear parts see Fu 2008.

4. Den Hartog tuning in analogy to mechanical damper

Since the modes of the main structure seem to be sufficiently separated, modal tuning of TLCGD is performed by a transformation of the classical Den Hartog formulas by means of the analogy between TMD and TLCGD. This procedure needs to approximately isolate a single mode of the structure, with TLCGD (or TMD) added, a two-DOF system results subjected to optimization. The analogy to TMD tuning is properly worked out.

Optimal TMD design parameters, frequency ratio and damping coefficient, are determined subjected to the harmonic excitation. The optimum tuning frequency ratio between the equivalent mechanical absorber and the main structure for minimum total acceleration is, see Den Hartog 1956, page 97 and 101,

$$\delta_{opt}^* = \frac{1}{1 + \mu^*} \tag{14}$$

and the corresponding optimum linear viscous damping coefficient is given by

$$\zeta_{opt}^* = \sqrt{\frac{3\mu^*}{8(1 + \mu^*)}} \tag{15}$$

The same parameters apply also in case of time harmonic forcing and minimizing the dynamic displacement magnification factor of the main system.

4.1 TMD attached to floor numbered *i*

Considering the passive spring-mass-damper at the same position in the same floor attached, sketched in Fig. 5 renders by the standard analysis Eqs. (16) and (17). All parameters are denoted by an asterisk to refer to the tuned mechanical damper.

$$\ddot{u}^* + 2\zeta_A^* \omega_A^* \dot{u}^* + \omega_A^{*2} u^* = -[\ddot{v}_g + \ddot{v}_i - (z_{Ai} - z_{C_{Mi}})\ddot{\theta}_i] \cos \gamma - [\ddot{w}_g + \ddot{w}_i + (y_{Ai} - y_{C_{Mi}})\ddot{\theta}_i] \sin \gamma \tag{16}$$

$$\begin{aligned} F_{Aiy}^* &= m_A^* [\ddot{v}_g + \ddot{v}_i - (z_{Ai} - z_{C_{Mi}})\ddot{\theta}_i] + m_A^* \ddot{u}^* \cos \gamma \\ F_{Aiz}^* &= m_A^* [\ddot{w}_g + \ddot{w}_i + (y_{Ai} - y_{C_{Mi}})\ddot{\theta}_i] + m_A^* \ddot{u}^* \sin \gamma, \quad M_{Aix}^* \approx 0 \end{aligned} \tag{17}$$

Eqs. (16) and (17) are the TMD counterparts of Eqs. (9), (10) and (12).

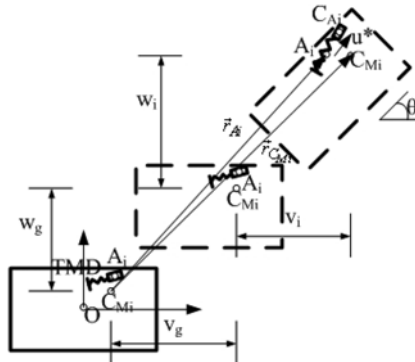


Fig. 5 TMD under general in-plane acceleration of the floor: \ddot{v}_i, \ddot{w}_i and $\ddot{\theta}_i$

4.2 Substructure synthesis of TLCDG/ TMD to the main system

Preparation of the linear tuning procedure requires the linearized equation of the projected main system with the absorber synthesized. The modal matrix of the main system is assumed known and the absolute floor displacements of the selected mode numbered j , $v_i = q_j \phi_{j(3i-2)}$, $w_i = q_j \phi_{j(3i-1)}$, $u_{Ti} = r_{Si} \theta_i = q_j \phi_{j3i}$, are substituted in the control forces of the resulting system and in the absorber Eqs. (9) and (16) as well, assuming the natural frequencies to be well separated. The approximated modal matrix equation of motion for the coupled system considering the multi-storey building with the TLCDG/TMD becomes, forced by an oblique single point base excitation $\vec{x}_g = [\ddot{v}_g, \ddot{w}_g]^T$ and by wind forces $\vec{F}(t)$,

$$\begin{bmatrix} 1 + \mu_j & \bar{\kappa}(v_{Aij} \cos \gamma + w_{Aij} \sin \gamma) m_{fj} / m_j \\ \kappa(v_{Aij} \cos \gamma + w_{Aij} \sin \gamma) & 1 \end{bmatrix} = \begin{bmatrix} \ddot{q}_j \\ \ddot{u} \end{bmatrix} + \begin{bmatrix} 2\zeta_{Sj} \omega_{Sj} & 0 \\ 0 & 2\zeta_{Aj} \omega_{Aj} \end{bmatrix} \begin{bmatrix} \dot{q}_j \\ \dot{u} \end{bmatrix} + \begin{bmatrix} \omega_{Sj}^2 & 0 \\ 0 & \omega_{Aj}^2 \end{bmatrix} \begin{bmatrix} q_j \\ u \end{bmatrix} = \begin{bmatrix} \vec{L}_j^T / m_j \\ \kappa \vec{r}_S^T \end{bmatrix} \ddot{\vec{x}}_g + \begin{bmatrix} \vec{\phi}_j^T \vec{F}(t) / m_j \\ 0 \end{bmatrix} \quad (18)$$

$$\begin{bmatrix} 1 + \mu_j^* & (v_{Aij} \cos \gamma + w_{Aij} \sin \gamma) m_{Aj}^* / m_j^* \\ (v_{Aij} \cos \gamma + w_{Aij} \sin \gamma) & 1 \end{bmatrix} = \begin{bmatrix} \ddot{q}_j \\ \ddot{u}^* \end{bmatrix} + \begin{bmatrix} 2\zeta_{Sj}^* \omega_{Sj}^* & 0 \\ 0 & 2\zeta_{Aj}^* \omega_{Aj}^* \end{bmatrix} \begin{bmatrix} \dot{q}_j \\ \dot{u}^* \end{bmatrix} + \begin{bmatrix} \omega_{Sj}^{*2} & 0 \\ 0 & \omega_{Aj}^{*2} \end{bmatrix} \begin{bmatrix} q_j \\ u^* \end{bmatrix} = \begin{bmatrix} \vec{L}_j^{*T} / m_j^* \\ \vec{r}_S^T \end{bmatrix} \ddot{\vec{x}}_g + \begin{bmatrix} \vec{\phi}_j^T \vec{F}(t) / m_j^* \\ 0 \end{bmatrix} \quad (19)$$

$$\mu_j = m_{fj} V_{ij}^2 / m_j < 6\%, \mu_j^* = m_{Aj}^* V_{ij}^{*2} / m_j^*, V_{ij}^2 = V_{ij}^{*2} + \bar{\kappa}_3 (\phi_{j3i} H / r_{Si})^2$$

$$V_{ij}^{*2} = v_{Aij}^2 + w_{Aij}^2, v_{Aij} = \phi_{j(3i-2)} - \phi_{j3i} (z_{Aij} - z_{C_M}) / r_{Si}$$

$$w_{Aij} = \phi_{j(3i-1)} + \phi_{j3i} (y_{Aij} - y_{C_M}) / r_{Si}, \vec{r}_S^T = [\cos \gamma \quad \sin \gamma], \vec{L}_j^T = [L_{jy} \quad L_{jz}]$$

$$L_{jy} = \sum_{n=1}^N m_{Sn} \phi_{j(3n-2)} + m_{fj} v_{Aij}, L_{jz} = \sum_{n=1}^N m_{Sn} \phi_{j(3n-1)} + m_{fj} w_{Aij}, \vec{L}_j^{*T} = [L_{jy}^* \quad L_{jz}^*]$$

$$L_{jy}^* = \sum_{n=1}^N m_{Sn}^* \phi_{j(3n-2)} + m_{Aj}^* v_{Aij}, L_{jz}^* = \sum_{n=1}^N m_{Sn}^* \phi_{j(3n-1)} + m_{Aj}^* w_{Aij} \quad (20)$$

where μ_j , ζ_{Sj} , ω_{Sj} and ω_{Aj} are the generalized mass ratio, the light modal structural damping ($\zeta_{Sj} \ll 1$), the circular natural frequency of the main structure and the TLCDG's circular natural frequency, respectively. μ_j^* , ω_{Sj}^* and ω_{Aj}^* are the alternative mass ratio, the circular natural frequency of the equivalent structure and the equivalent TMD's circular natural frequency. m_{Sn} , m_{Sn}^* and m_j , m_j^* denote the mass of the floor number n and the modal mass, possibly unit. The modified participation factor \vec{L}_j , \vec{L}_j^* and the effective wind load $\vec{\phi}_j^T \vec{F}(t) / m_j$, $\vec{\phi}_j^T \vec{F}(t) / m_j^*$ are identified. v_{Aij}

and w_{Aij} denote the modal displacements of the reference point A_i in y - and z -directions, respectively. $m_f(1 - \kappa\bar{\kappa})$ must be regarded as the dead fluid mass, thus slightly reducing the natural frequency of the main structure. The dead mass of the piping system at this stage of the tuning procedure is neglected. It is taken into account during the fine tuning in state space.

4.3 Modal tuning by analogy to the equivalent TMD

Comparing the right hand side of the second equations in Eqs. (18) and (19), u^* turns out proportional to u considering the same excitation, $u^* = u/\kappa$. The mass ratio of the equivalent TMD-modal system by inspection of the first equations of Eqs. (18) and (19) and the TLCGD frequency ratio by the general transformation are identified, j refers to the mode number,

$$\mu_j^* = \mu_j \frac{\kappa\bar{\kappa}(V_{ij}^*/V_{ij})^2}{1 + \mu_j[1 - \kappa\bar{\kappa}(V_{ij}^*/V_{ij})^2]} < \mu_j, \quad \delta_{jopt} = \frac{f_{A_i,opt}}{f_{S_j}} = \frac{\delta_{jopt}^*}{\sqrt{1 + \mu_j[1 - \kappa\bar{\kappa}(V_{ij}^*/V_{ij})^2]}}, \quad \zeta_{A_j} = \zeta_{A_j}^* \quad (21)$$

Thus, the optimal frequency ratio δ_{jopt} of the TLCGD turns out slightly lowered. The optimal damping coefficient remains unchanged.

5. Optimization in the state space domain, in case of earthquake excitation

The asymmetric structure when subjected to wind forces, in-wind loading by wind gusts and lateral loading by vortex shedding etc., requires separate investigations in the state space. In this section the parameter optimization in state space for structure with several absorbers installed and considering a single point oblique base excitation is performed. The MDOF main system, a 3N-degree of freedom space frame building (with a number of N floors) considered, now with a number of $n \ll 3N$ TLCGDs at proper locations tuned to a consecutive number of low frequency modes, the linearized control forces at i -th storey produced by several TLCGDs takes on the matrix form,

$$\begin{aligned} \vec{F}_{Ai} = & - \underbrace{\begin{pmatrix} m_{i,tot} & 0 & z_i m_{i,tot}/r_{Si} \\ 0 & m_{i,tot} & y_i m_{i,tot}/r_{Si} \\ z_i m_{i,tot}/r_{Si} & y_i m_{i,tot}/r_{Si} & r_i^2 m_{i,tot}/r_{Si}^2 \end{pmatrix}}_{W_i} \underbrace{\begin{pmatrix} \ddot{v}_i + \ddot{v}_g \\ \ddot{w}_i + \ddot{w}_g \\ \ddot{u}_{Ti} \end{pmatrix}}_{\ddot{x}_i + \ddot{x}_g} \\ & - \underbrace{\begin{pmatrix} \dots & \bar{\kappa} \cos \gamma m_f & \dots \\ \dots & \bar{\kappa} \sin \gamma m_f & \dots \\ \dots & \bar{\kappa} [(y_{Ai} - y_{C_{M_i}}) \sin \gamma - (z_{Ai} - z_{C_{M_i}}) \cos \gamma] m_f & \dots \end{pmatrix}}_{W_{\bar{\kappa}}} \ddot{u} \\ z_i = & - \frac{\sum (z_{Ai} - z_{C_{M_i}}) m_f}{m_{i,tot}}, \quad y_i = \frac{\sum (y_{Ai} - y_{C_{M_i}}) m_f}{m_{i,tot}} \\ r_i^2 = & \frac{\sum [(y_{Ai} - y_{C_{M_i}})^2 + (z_{Ai} - z_{C_{M_i}})^2 + \bar{\kappa}_3 H^2] m_f}{m_{i,tot}} \end{aligned} \quad (22)$$

where $m_{i, tot}$ is the total mass of the installed TLCGDs on the i -th floor. In case there no TLCGDs installed the control forces are zero.

The equations of motion for TLCGD-main structure system by substituting the control force and rearranging terms, can be given as, single point excitation of the base understood,

$$\underbrace{\begin{bmatrix} \tilde{\mathbf{M}} + \tilde{\mathbf{W}} & \tilde{\mathbf{W}}_{\tilde{\mathbf{x}}} \\ \tilde{\mathbf{e}} & \tilde{\mathbf{I}} \end{bmatrix}}_{\tilde{\mathbf{M}'}} + \begin{bmatrix} \tilde{\ddot{\mathbf{x}}} \\ \tilde{\ddot{\mathbf{u}}} \end{bmatrix} + \begin{bmatrix} \tilde{\mathbf{C}} & \tilde{\mathbf{0}} \\ \tilde{\mathbf{0}} & \tilde{\mathbf{C}}_f \end{bmatrix} \begin{bmatrix} \dot{\tilde{\mathbf{x}}} \\ \dot{\tilde{\mathbf{u}}} \end{bmatrix} + \begin{bmatrix} \tilde{\mathbf{K}} & \tilde{\mathbf{0}} \\ \tilde{\mathbf{0}} & \tilde{\mathbf{K}}_f \end{bmatrix} \begin{bmatrix} \tilde{\mathbf{x}} \\ \tilde{\mathbf{u}} \end{bmatrix} = \begin{bmatrix} \tilde{\mathbf{M}} + \tilde{\mathbf{W}} \\ \tilde{\mathbf{e}} \end{bmatrix} \tilde{\mathbf{E}}_N \ddot{\tilde{\mathbf{x}}}_g$$

$$\mathbf{e}_i = \begin{pmatrix} \dots & \kappa \cos \gamma & \dots \\ \dots & \kappa \sin \gamma & \dots \\ \dots & (y_{Ai} - y_{C_{M_i}}) \kappa \sin \gamma - (z_{Ai} - z_{C_{M_i}}) \kappa \cos \gamma & \dots \end{pmatrix}^T, \tilde{\mathbf{E}}_N = \begin{bmatrix} 1 & 0 & 0 & 1 & 0 & 0 & 1 & \dots \\ 0 & 1 & 0 & 0 & 1 & 0 & 0 & \dots \end{bmatrix} \quad (23)$$

$\tilde{\mathbf{M}}$ denotes the diagonal mass matrix, containing three lumped mass elements per floor. $\tilde{\mathbf{C}}$ and $\tilde{\mathbf{K}}$ are light damping (even non classical) and stiffness matrices of the main system. $\tilde{\mathbf{x}}^T = [v_1, w_1, u_{T1}, \dots, v_N, w_N, u_{TN}]^T$ means the displacement vector in the center of mass of the N -storey building, $u_{TN} = \theta_N r_{SN}$. $\ddot{v}_g = a_g \cos \alpha$, $\ddot{w}_g = a_g \sin \alpha$ in $\ddot{\tilde{\mathbf{x}}}_g = [\ddot{v}_g, \ddot{w}_g]^T$ are the components of the obliquely incident ground acceleration $a_g(t)$, while soil-structure interaction is neglected. $\tilde{\mathbf{C}}_f$ and $\tilde{\mathbf{K}}_f$ are the linearized damping matrix and the ‘‘stiffness’’ matrix of TLCGDs, $\tilde{\mathbf{u}}^T = [u_1 \dots u_n]$ samples the relative fluid displacements of n TLCGDs.

To make the tools of control theory applicable, this system of second order differential equation can be lastly converted to a first order state space representation by introducing the state hyper vector $2(3N + n)$, $\tilde{\mathbf{z}} = [\tilde{\dot{\mathbf{x}}}^T \tilde{\dot{\mathbf{u}}}^T \tilde{\mathbf{x}}^T \tilde{\mathbf{u}}^T]^T$ and its time derivative, see e.g., Ziegler 1998, page 438

$$\dot{\tilde{\mathbf{z}}} = (\tilde{\mathbf{A}} + \tilde{\mathbf{B}}\tilde{\mathbf{R}})\tilde{\mathbf{z}} + \tilde{\mathbf{e}}_g \ddot{\tilde{\mathbf{x}}}_g(t) \quad (24)$$

where, in a hypermatrix notation, the system matrix remains separated,

$$\tilde{\mathbf{A}} = \begin{bmatrix} \tilde{\mathbf{0}} & \tilde{\mathbf{0}} & \tilde{\mathbf{I}} & \tilde{\mathbf{0}} \\ \tilde{\mathbf{0}} & \tilde{\mathbf{0}} & \tilde{\mathbf{0}} & \tilde{\mathbf{I}} \\ -\tilde{\mathbf{M}}'^{-1} \begin{bmatrix} \tilde{\mathbf{K}} & \tilde{\mathbf{0}} \\ \tilde{\mathbf{0}} & \tilde{\mathbf{0}} \end{bmatrix} & -\tilde{\mathbf{M}}'^{-1} \begin{bmatrix} \tilde{\mathbf{C}} & \tilde{\mathbf{0}} \\ \tilde{\mathbf{0}} & \tilde{\mathbf{0}} \end{bmatrix} & & \end{bmatrix}, \tilde{\mathbf{B}} = \begin{bmatrix} \tilde{\mathbf{0}} & \tilde{\mathbf{0}} & \tilde{\mathbf{0}} & \tilde{\mathbf{0}} \\ \tilde{\mathbf{0}} & \tilde{\mathbf{0}} & \tilde{\mathbf{0}} & \tilde{\mathbf{0}} \\ -\tilde{\mathbf{M}}'^{-1} \begin{bmatrix} \tilde{\mathbf{I}} & \tilde{\mathbf{0}} \\ \tilde{\mathbf{0}} & \tilde{\mathbf{I}} \end{bmatrix} & -\tilde{\mathbf{M}}'^{-1} \begin{bmatrix} \tilde{\mathbf{I}} & \tilde{\mathbf{0}} \\ \tilde{\mathbf{0}} & \tilde{\mathbf{I}} \end{bmatrix} & & \end{bmatrix}$$

$$\tilde{\mathbf{R}} = \begin{bmatrix} \tilde{\mathbf{0}} & \tilde{\mathbf{0}} & \tilde{\mathbf{0}} & \tilde{\mathbf{0}} \\ \tilde{\mathbf{0}} & \tilde{\mathbf{K}}_f & \tilde{\mathbf{0}} & \tilde{\mathbf{0}} \\ \tilde{\mathbf{0}} & \tilde{\mathbf{0}} & \tilde{\mathbf{0}} & \tilde{\mathbf{0}} \\ \tilde{\mathbf{0}} & \tilde{\mathbf{0}} & \tilde{\mathbf{0}} & \tilde{\mathbf{C}}_f \end{bmatrix}, \tilde{\mathbf{e}}_g = \begin{bmatrix} \tilde{\mathbf{0}} \\ \tilde{\mathbf{0}} \\ -\tilde{\mathbf{M}}'^{-1} \begin{bmatrix} \tilde{\mathbf{M}} + \tilde{\mathbf{W}} \\ \tilde{\mathbf{e}} \end{bmatrix} \tilde{\mathbf{E}}_N \end{bmatrix} \quad (25)$$

The state space will turn out to be very effective in the following parameter optimization. All absorber tuning parameters are included in parameter matrix $\tilde{\mathbf{R}}$, whose diagonal sub-matrices $\tilde{\mathbf{C}}_f$

and \underline{K}_f must have positive valued diagonal elements to ensure passivity and stability of the system. Assuming the ground excitation to be time-harmonic

$$\ddot{\vec{x}}_g(t) = \begin{Bmatrix} \ddot{v}_g(t) \\ \ddot{w}_g(t) \end{Bmatrix} = a_0 \vec{e}_s e^{i\omega t}, \quad \vec{e}_s^T = [\cos \alpha \sin \alpha] \quad (26)$$

The complex time-harmonic solution simply becomes, α is the angle of attack of the earthquake,

$$\vec{z}(\alpha, \omega) = [i\omega \underline{I} - (\underline{A} + \underline{B}\underline{R})]^{-1} \underline{e}_g \vec{e}_s a_0 \quad (27)$$

The optimal natural frequencies and the damping ratios of the absorbers are calculated by minimizing the following performance index, corresponding to the minimum of the area under the resonance curve,

$$J = \int_{-\infty}^{\infty} \vec{z}_s^T(\omega) \underline{S} \vec{z}_s(\omega) d\omega = 2\pi \bar{b}^T \underline{P} \bar{b} \rightarrow \text{Minimum}, \quad \vec{z}_s = [\vec{x} \quad \dot{\vec{x}}]^T \quad (28)$$

where \vec{z}_s represents the state vector $6N \times 1$ of the main structure. The positive semidefinite weighing matrix \underline{S} is chosen e.g., to pronounce displacements. $\bar{b} = \underline{e}_g \vec{e}_s a_0$ is the excitation vector. \underline{P} is consequently the solution of the algebraic Lyapunov matrix equation, $(\underline{A} + \underline{B}\underline{R})^T \underline{P} + \underline{P}(\underline{A} + \underline{B}\underline{R}) = -\underline{S}$, see Hochrainer 2001. The latter is numerically evaluated by means of the software MATLAB 2002. The minimization of J is performed numerically by calling the function *fminsearch* of the Matlab Optimization Toolbox. *fminsearch* finds the minimum of the scalar function J of several variables quickly when Den Hartog's modal tuning parameters are substituted for the initial estimates. Especially, the dividing of a TLCGD with a much too large cross-sectional area into smaller units in parallel action, requires fine tuning for practical applications, Fu 2008.

6. Applications of passive TLCGD to buildings

Since an impressive increase of the effective modal damping over the light structural damping by the action of the TLCGD, the reduction of the response to wind excitation seems to be quite naturally given. The full simulations of the linearized system (structure with TLCGDs attached) are given for seismic excitation. There is no explicit need to repeat such simulations for the wind load.

6.1 Single-storey asymmetric space-frame

The commonly uniformly distributed mass of the floor with rectangular plan $a \times b = 8 \times 4$ m is $m_s = 16 \times 10^4$ kg and an eccentric point mass $m_1 = 6 \times 10^3$ kg is considered placed in the corner $A_1(4, 2, 0)$ in Fig. 1. The common anisotropic stiffness of column in each corner in y - and z -directions are $k_y = 981.2$ kN/m and $k_z = 350$ kN/m. The natural frequencies are 1.16, 1.96 and 2.37 Hz. With the three modal centers of velocity considered, all are outside of the floor plan, Fig. 6 shows the arrangement of the three TLCGDs (constant cross-sectional area of the pipe is assumed), tuned with respect to the corresponding natural frequencies.

The fluid mass is chosen as $m_{f1} = 770$ kg, $m_{f2} = 320$ kg and $m_{f3} = 180$ kg of water. Dimensions of the three TLCGDs are summarized in Table 1. They are at first modally tuned by means of the

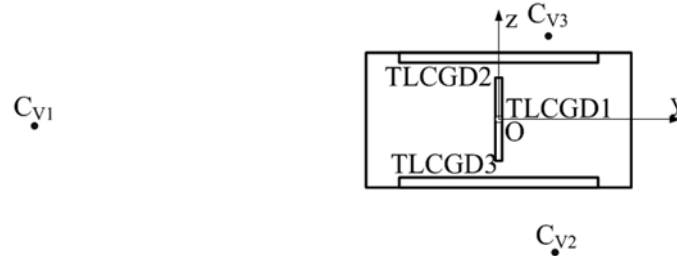


Fig. 6 Installation of three TLCGDs in a single-storey asymmetric building. • indicates the centers of velocity C_{vj}

Table 1 Layout of the modally tuned TLCGDs, gas volume selected and gas equilibrium pressure assigned, Fig. 6

| | TLCGD 1 | TLCGD 2 | TLCGD 3 | |
|---|----------------------|----------|----------|------|
| Horizontal length of the liquid column B [m] | 3.00 | 2.50 | 3.00 | |
| Inclined length of the liquid column H [m] | 1.40 | 0.86 | 0.60 | |
| Cross-sectional area of the pipe [m ²] | 0.1330 | 0.0760 | 0.0430 | |
| Effective length $L_{eff} = L_1 = 2H + B$ [m] Eqs. (7) (11) | 5.80 | 4.22 | 4.20 | |
| Angle of the inclined pipe section β [rad] | $\pi/4$ | $\pi/4$ | $\pi/4$ | |
| Geometry factor $\kappa = \bar{\kappa}$ Eqs. (7),(11) | 0.86 | 0.88 | 0.92 | |
| Geometry factor $\bar{\kappa}_3$ Eq. (13) | 1.20 | 1.77 | 3.83 | |
| Equilibrium pressure head h_0 , [m] $n = 1.2$, Eq. (8) | 36.70 | 45.26 | 46.50 | |
| Gas volume $V_0 = A_H H_a$ [m ³] Eq. (5) | 0.340000 | 0.110000 | 0.044000 | |
| Natural frequency f_{Aopt} [Hz] | Den Hartog Eq. (14) | 1.13 | 1.92 | 2.33 |
| | Fine tuning Eq. (28) | 1.13 | 1.90 | 2.33 |
| Optimum linear damping % | Den Hartog Eq. (15) | 8.96 | 7.37 | 6.68 |
| | Fine tuning Eq. (28) | 7.51 | 5.72 | 4.91 |

TMD analogy, Eq. (21), and by substituting Den Hartog's formulas, see again Eqs. (14) and (15). Subsequently, a fine-tuning process in state space is performed, Eq. (28). Optimal frequencies remain nearly unchanged and damping is dramatically lowered. By the action of the three TLCGDs, the effective modal damping coefficients of the system in each mode are increased from 1% to 5.9, 4.77 and 4.34%. Varying the angle of attack of the time harmonic base acceleration, strength 0.1 g, the weighed sum of the frequency response functions of the original and the optimized system was calculated using MATLAB 2002. The maximum gain from all three TLCGDs is exemplarily made visible with a selected simulation ($\alpha = \pi/6$) in Fig. 7. It is obvious that the parameter optimization reduced the vibration amplitude at the resonant peaks tremendously. The maximum relative fluid strokes for all cases are within the design limits, Fig. 8. The maximum relative fluid speed is well below the limit given in Lindner-Silvester and Schneider 2005, $\omega_{Aj}|u_{max,j}| < 10$ m/s, $j = 1, 2, 3$. The detailed TLCGDs design and the simulation results see Fu 2008.

The seismic acceleration record of the 1940 NS-EI Centro earthquake ($a_0 = 0.35$ g) with the angle of attack α is applied to this structure. The three TLCGDs with fine-tuning parameters are considered in their linearized modal damping assigned. One illustrative result of the simulations is

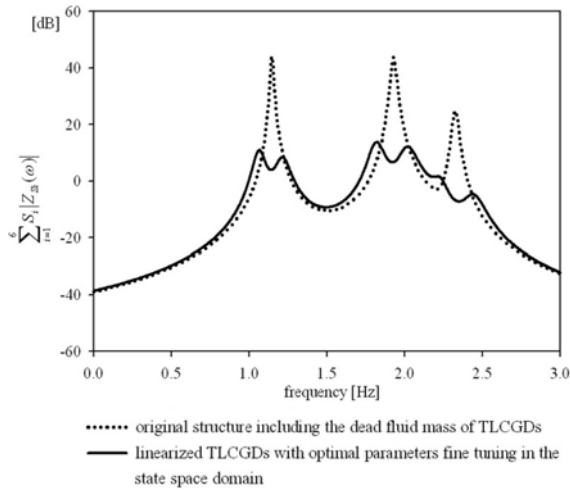


Fig. 7 Weighed sum of amplitude response functions for the 3-DOF, linearized, single-storey, asymmetric space frame, without/with three linearized TLCGDs attached. Angle of attack of the time-harmonic base acceleration, $a_0 = 0.1 \text{ g}$, $\alpha = \pi/6$. Maximum gain 30 dB

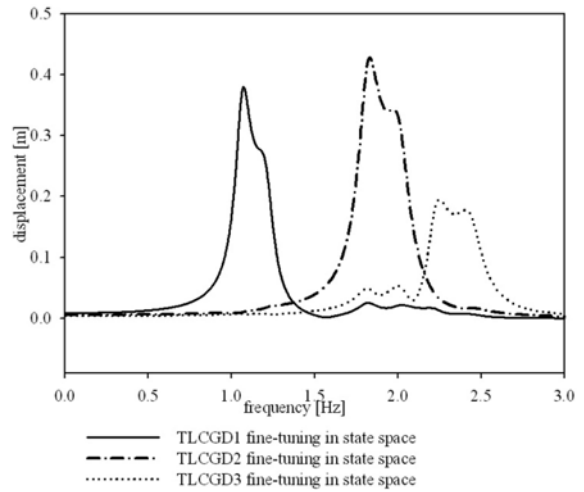


Fig. 8 Amplitude response curves of the relative fluid motion in three TLCGDs attached to the single-storey, asymmetric space frame. Angle of attack $\alpha = \pi/6$. Larger relative fluid strokes result after fine-tuning as a consequence of the lowered optimal damping

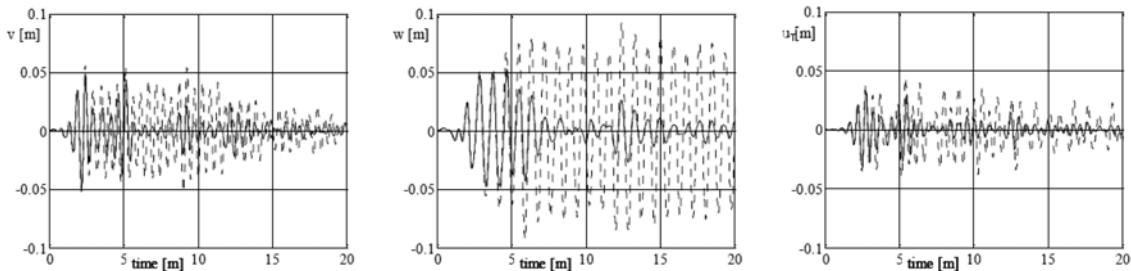


Fig. 9 Relative floor displacements of center of mass, v , w , and rotation $u_T = r_S \theta$, $r_S = 2.97 \text{ m}$. 1940 El Centro earthquake, strong motion phase 20s, angle of attack: $\alpha = \pi/6$ --- without TLCGDs, — with TLCGDs

shown in Fig. 9. However, the maximum accelerations, peaking at early times within the strong motion phase, are hardly affected. Their reduction requires active control rendering the TLCGD hybrid, the ATLTCGD, see Hochrainer 2001 for a design proposal.

6.2 Four-storey asymmetric building

The same mass of each floor $16 \times 10^3 \text{ kg}$ with the different point mass ($6 \times 10^3 \text{ kg}$, $8 \times 10^3 \text{ kg}$, $10 \times 10^3 \text{ kg}$ and $6 \times 10^3 \text{ kg}$) orderly placed in the corner causes the centers of mass of the floors not on vertical axes. The common stiffness of columns are increased from section 6.1 to $k_{yi} = 5874.4 \text{ kN/m}$ and $k_{zi} = 2021.9 \text{ kN/m}$. The computed first four natural frequencies are 0.97, 1.61, 2.01 and 2.88 Hz. With the first four modal centers of velocity considered, the possible arrangements of

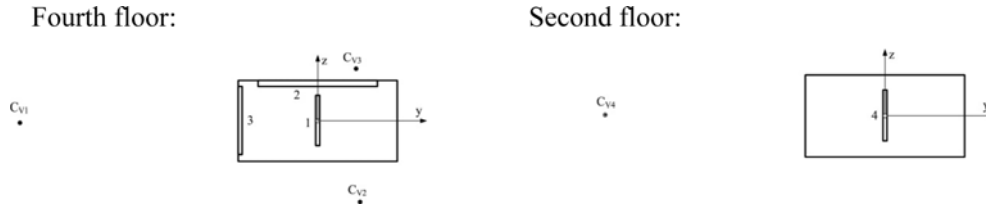


Fig. 10 Installation of TLCGDs, \odot the centers of velocity of second floor, \bullet the centers of velocity of fourth, top floor. Scaled figures

Table 2 Layout of the modally tuned TLCGDs, gas volume selected and gas equilibrium pressure assigned, Fig. 10

| | TLCD 1 | TLCD 2 | TLCD 3 | TLCD 4 | |
|---|----------------------|----------|----------|----------|------|
| Horizontal length of the liquid column B [m] | 3.00 | 3.00 | 3.00 | 3.50 | |
| Inclined length of the liquid column H [m] | 2.40 | 1.40 | 1.40 | 0.50 | |
| Cross-sectional area of the pipe [m ²] | 0.2600 | 0.1400 | 0.0480 | 0.0880 | |
| Effective length $L_{eff} = L_1 = 2H + B$ [m] Eqs. (7) (11) | 7.80 | 5.80 | 5.80 | 4.50 | |
| Angle of the inclined pipe section β [rad] | $\pi/4$ | $\pi/4$ | $\pi/4$ | $\pi/4$ | |
| Geometry factor $\kappa = \bar{\kappa}$ Eqs. (7),(11) | 0.82 | 0.859 | 0.876 | 0.935 | |
| Geometry factor $\bar{\kappa}_3$ Eq. (13) | 0.665 | 1.198 | 1.623 | 6.485 | |
| Equilibrium pressure head h_0 , [m] $n = 1.2$, Eq. (8) | 56.28 | 69.72 | 86.88 | 88.08 | |
| Gas volume $V_0 = A_H H_a$ [m ³] Eq. (5) | 1.040000 | 0.330000 | 0.100000 | 0.110000 | |
| Natural frequency f_{Aopt} [Hz] | Den Hartog Eq. (14) | 0.945 | 1.585 | 1.982 | 2.86 |
| | Fine tuning Eq. (28) | 0.941 | 1.552 | 1.893 | 2.86 |
| Optimum linear damping % | Den Hartog Eq. (15) | 8.50 | 7.16 | 6.35 | 4.08 |
| | Fine tuning Eq. (28) | 7.81 | 5.75 | 5.81 | 3.62 |

absorbers are illustrated in Fig. 10. The top floor is suitable to host all modally TLCGDs. For the fourth mode, the second floor with the largest modal displacement becomes suitable. The fluid mass $m_{f1} = 2030$ kg, $m_{f2} = 810$ kg, $m_{f3} = 250$ kg and $m_{f4} = 400$ kg of water are selected for four TLCGDs. Dimensions of the TLCGDs are summarized in Table 2. The effective modal damping coefficients of the system are increased from 1% to 5.6, 4.67, 4.2 and 3.1%.

Numerical studies have been performed for various angles of attack of the ground motion $\alpha_0 = 0.1$ g, with a selected simulation shown, $\alpha = \pi/6$. The maximum gain from all TLCGDs is exemplarily made visible in Fig. 11 with the relative fluid strokes plotted in Fig. 12. The resonance curves with fine-tuned optimal parameters understood, have broader peaks. The gain due to the increase of the effective structural damping is impressive.

One illustrative result of the simulations of the four-storey asymmetric space frame under the NS-El Centro earthquake is shown in Fig. 13, where the relative floor displacements with respect to the base and the relative floor accelerations in terms of the root mean square (RMS) values are displayed. The RMS value is defined by

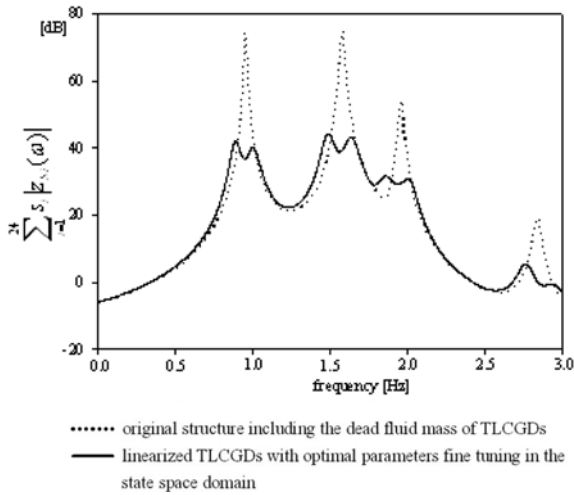


Fig. 11 Weighed sum of amplitude response functions for the four-storey, asymmetric space frame, without/with four linearized TLCGDs attached (angle of attack of the time-harmonic base acceleration: $a_0 = 0.1$ g, $\alpha = \pi/6$). Maximum gain 30.7 dB

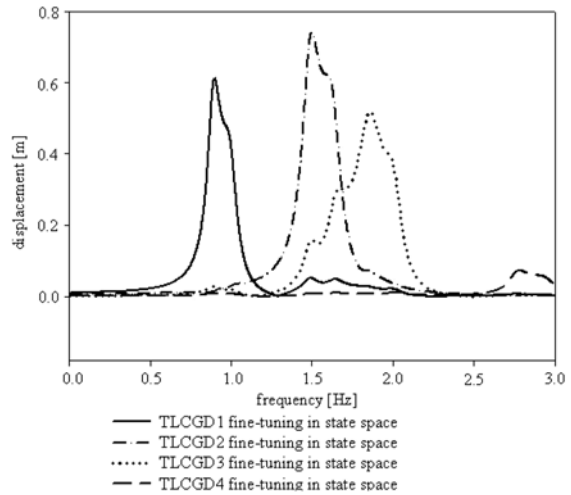


Fig. 12 Amplitude response curves of the relative fluid motion in four TLCGDs attached to the four-storey, asymmetric space frame. Angle of attack $\alpha = \pi/6$

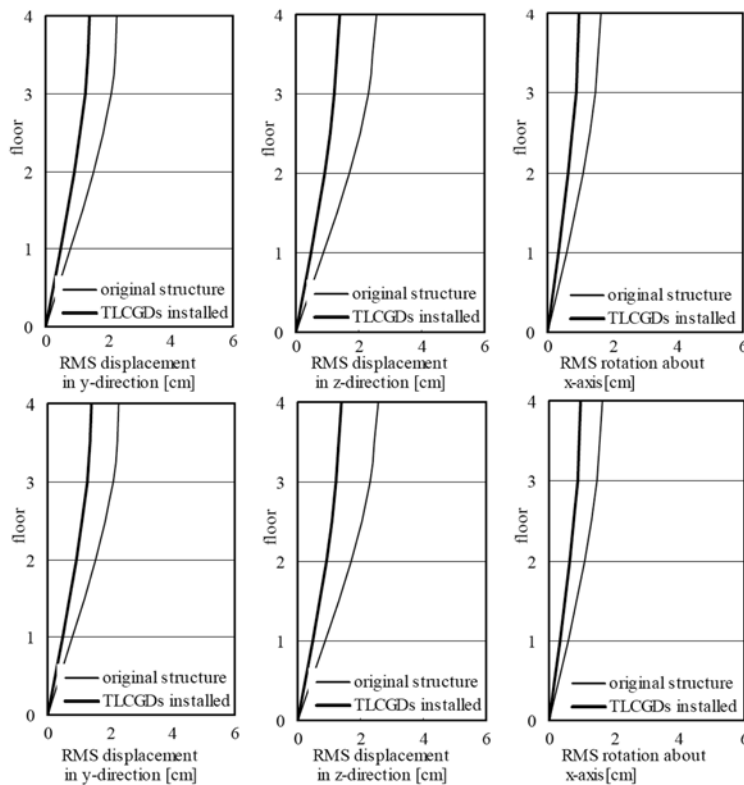


Fig. 13 RMS response of the relative floor displacement and of the relative floor acceleration of the four-storey asymmetric building (El Centro, 0.35 g, angle of attack $\alpha = \pi/6$)

$$RMS = \sqrt{\frac{1}{t_S} \int_0^{t_S} \dot{u}^2 dt}, \quad t_S = 20s \quad (29)$$

where t_S is the strong motion phase of the NS-EI Centro earthquake record.

The rotation displacement about x -axis is $u_{Ti} = \theta r_{Si}$, where $r_{S1} = 2.97$ m, $r_{S2} = 2.98$ m, $r_{S3} = 2.97$ m, $r_{S4} = 2.97$ m. It is seen that the RMS response is impressively reduced by the increased effective structural damping. Thus, it is concluded that the optimally tuned absorbers are adequate for effective damping of asymmetric buildings in seismic active zones.

7. Conclusions

The tuned liquid column gas damper (TLCGD) is well suited to mitigate wind- and earthquake excited dominating horizontal vibrations of plan-asymmetry buildings assumed a three DOF at each floor, equally as well as an increase of the modal structural damping. Its optimum installation location requires the largest allowable normal distance to the modal center of velocity in the floor with large modal displacements, when this center lies outside of the floor plan. The equation of the relative fluid flow in a sealed TLCGD uses the extended non-stationary Bernoulli equation for moving reference systems. The interaction force and moment between TLCGD and the main structure are assigned. Starting from the linearized equations a geometric analogy between TMD and TLCGD is worked out which allows the transformations of the optimization parameters (Den Hartog formula) of the TMD to TLCGD. The gas-spring effect in the sealed TLCGD extends the frequency range of application. The adjustable equilibrium gas pressure becomes an easily accessible tuning parameter. A sufficient condition based on the cut-off damping coefficient of parametric resonance allows neglecting the effects of the vertical or rotational motion. In order to keep the fluid-gas interface intact, the allowable relative speed of the fluid must be limited by about 10 m/s. Consequently, it is pointed out the first time that for a given maximum fluid stroke the frequency range of application becomes equally limited.

Acknowledgements

The Fellowship received from the *Afro Asiatisches Institut* (AAI) in Vienna for the years 2005-2008 of PHD- studies at the Vienna University of Technology is gratefully acknowledged.

References

- DenHartog, J.P. (1956), *Mechanical Vibrations*, Repr. 4th ed, McGraw-Hill, New York.
- Fu, C. (2008), "Effective damping of vibrations of plan-asymmetric buildings", *Dissertation, Vienna University of Technology, Austria*, <http://www.tuwien.ac.at/>.
- Hitchcock, P.A., Kwok, K.C., Watkins, R.D. and Samali, B. (1997), "Characteristics of liquid column vibration absorbers (LCVA)-II", *Eng. Struct.*, **19**, 135-144.
- Hitchcock, P.A., Kwok, K.C., Watkins, R.D. and Samali, B. (1997), "Characteristics of liquid column vibration absorbers (LCVA)-I", *Eng. Struct.*, **19**, 126-134.

- Hochrainer, M.J. (2001), "Control of vibrations of civil engineering structures with special emphasis on tall buildings", *Dissertation, Vienna University of Technology, Austria*, <http://www.tuwien.ac.at/>.
- Hochrainer, M.J. and Ziegler, F. (2006), "Control of tall building vibrations by sealed tuned liquid column dampers", *Struct. Control Health Monitor.*, **13**, 980-1002.
- Hochrainer, M.J. (2005), "Tuned liquid column damper for structural control", *Acta Mech.*, **175**, 57-76.
- Lindner-Silvester, T. and Schneider, W. (2005), "The moving contact line with weak viscosity effects – an application and evaluation of Shikhmurzaev's model", *Acta Mech.*, **176**, 245-258.
- MATLAB (2002), *User Guide, Control Toolbox*, MathWorks Inc., Version 6.5.1.
- Reiterer, M. (2004), "Damping of vibration-prone civil engineering structures with emphasis on bridges", *Dissertation (in German), Vienna University of Technology, Austria*, <http://www.tuwien.ac.at/>.
- Reiterer, M. and Ziegler, F. (2004), "Bi-axial seismic activation of civil engineering structures equipped with tuned liquid column dampers", *J. Seismol. Earthq. Eng.*, **6**(3), 45-60.
- Reiterer, M. and Ziegler, F. (2006), "Control of pedestrian-induced vibrations of long-span bridges", *Struct. Control Health Monitor.*, **13**, 1003-1027.
- Sakai, F., Takaeda, S. and Tamaki, T. (1989), "Tuned liquid column damper-new type device for suppression of building vibration", *Proc. Int. Conf. on High-rise Buildings*, Nanjing, China, 926-931.
- Ziegler, F. (1998), *Mechanics of Solids and Fluids*, corr. Repr. 2nd ed. Springer, New York.
- Ziegler, F. and Fu, C. (2007), "Effective vibration damping of plan-asymmetric buildings", *Proc. of the 8th Int. Conf. on Multi-purpose High-rise Towers and Tall Buildings* (Sabouni, A.-R.R., El-Sawy, K.M., eds.), The International Federation of High-Rise Structures. Abu Dhabi. CD-Rom Paper ID IFHS-039, 1-13. (www.acevents.ae 'online documents'_ifhs2007+ifhs2007dxb_TB-28.pdf).